Asteroidal Heating and Thermal Stratification of the Asteroid Belt

A. Ghosh
University of Tennessee and NASA Goddard Space Flight Center

S. J. Weidenschilling
Planetary Science Institute

H. Y. McSween Jr.
University of Tennessee

A. Rubin
University of California, Los Angeles

The asteroid belt is thermally stratified, with melted or metamorphosed asteroids dominating the inner belt and relatively unaltered asteroids dominating the outer belt. The compositional structure of the asteroid belt is a unique signature of the heating agent that caused melting and metamorphism of planetesimals in the early solar nebula, thus it constitutes an important test of plausibility of heating mechanisms. Previous work attributes the stratification to a radial thermal gradient in the solar nebula or heating by ^{26}Al decay or electromagnetic induction. Present thinking attributes the thermal stratification of multiple processes that were active in the early solar system, including ^{26}Al, the dependence to accretion timescale on heliocentric distance, the presence of ice in planetesimals that formed in the outer belt, and loss of primitive material by collisional disruption of small asteroids over the age of the solar system.

1. HEAT SOURCES IN THE EARLY SOLAR SYSTEM

Half a century ago, H. Urey recognized that "it is difficult to believe that heating by K, U and Th is a feasible explanation for the high-temperature stage required to produce the meteorites." He proceeded to perform the first back-of-the-envelope calculation and suggested ^{26}Al to be a heat source for asteroidal heating (*Urey,* 1955), and perhaps inadvertently initiated the subdiscipline of asteroid thermal modeling. Ever since, thermal models have been used as plausibility calculations for chondrite metamorphism (or melting) in an asteroidal body. Since Urey advocated ^{26}Al as a heat source, many heat sources have been suggested at various points of time in the literature, like the radiant energy of a Hayashi-phase Sun (*Wasson,* 1974) and the energy released from exothermic reactions between unstable presolar compounds (*Clayton,* 1980). Of the proposed heat sources, three remain a subject of active discussion today: heating by the decay of ^{26}Al, electromagnetic induction, and impact heating.

1.1. Electromagnetic Induction Heating

The theory of electromagnetic induction heating, first proposed by *Sonnett et al.* (1968), was based on the physics of T Tauri outflow (*Kuhi,* 1964). An electric current is generated in planetesimals that move through an embedded magnetic field generated by the T Tauri phase of the Sun. This electric current that flows through the planetesimals causes them to undergo heating. There are two modes of electromagnetic induction: the transverse magnetic mode, which is caused by the steady motion of the solar wind past the planetesimals, and the transverse electric mode of heating, which is caused by the fluctuations in the magnetic field of the solar wind. The transverse magnetic mode is believed to be effective for asteroidal bodies (*Sonett and Colburn,* 1968; *Sonett et al.,* 1968), while the transverse electric mode is effective for larger bodies like the Moon. At the time of publication of the *Sonnett et al.* (1968) paper, the mass loss rates were believed to be very high: on the order of 50% of the initial mass of the Sun over the entire T Tauri phase. The T Tauri outflow was also believed to have been isotropic.

Modeling electromagnetic induction heating is fairly complex: This is reflected by the fact that remarkably few attempts have been made to model the phenomenon, in comparison to ^{26}Al heating models. It is straightforward to list the factors that will influence the degree of heating; it is simulating the relative importance and interdependence of the factors in the heating process that is difficult, particularly since a few of the variable parameters are unconstrained. The intensity as well as duration of the solar wind during the T Tauri phase determines the amount of current generated in the planetesimal, and therefore the amount of heating. Solar wind velocity, electrical conductivity, surface

magnetic field, and rotation rate of the T Tauri Sun are all proportional to the amount of heat generated. The size of a planetesimal is a more complicated parameter: It seems that the transverse magnetic (TM) mode in large bodies creates secondary magnetic fields strong enough to deflect part of the magnetic fields that can deflect part of the solar wind, thereby causing the induced electrical current to decrease. Thus, heating increases with asteroidal size until a critical radius is reached, beyond which an increase in size causes the heating to decrease.

Recent studies of T Tauri stars, however, moderate the conditions that would favor the electromagnetic induction heating hypothesis. First, the T Tauri stellar winds have been found to be anisotropic with a greater wind density at high latitudes, avoiding the plane of the circumstellar disk where planetesimals form (*Edwards et al.,* 1987). This goes against the assumption of isotropic dissipation of the solar wind by *Sonett et al.* (1968) and means that the solar wind flux in the equatorial plane where planets form was probably lower than was originally thought. Second, pre-main-sequence mass loss from a T Tauri star has been revised from ~50% (*Kuhi,* 1964) to a few percent (*DeCampli,* 1981), and the rate of mass loss has been revised downward by 1 to 2 orders of magnitude. Consequently, since the intensity of electromagnetic heating is proportional to the intensity of the solar wind (which in turn is governed by the rate of mass loss from the Sun), the amount of heat generation will also be lower than the initial models of *Sonett et al.* (1968). Third, it was believed that T Tauri outflow continued after planetesimals accreted and the disk dissipated. However, *Edwards et al.* (1987) showed that this phase does not exist; in other words, the T Tauri outflow stops as soon as the process of active accretion stops in the disk.

Recent models (*Herbert,* 1989; *Shimazu and Terasawa,* 1995) produce melting in asteroidal-sized bodies. However, this has not been without criticism; for example, *Wood and Pellas* (1991) analyze the parameters used by *Herbert et al.* (1991) and deduce that the latter do not take into account poleward collimation of the solar wind and assume higher-than-defensible values of solar wind velocities. The problem of electromagnetic induction heating hinges on the choice of a reasonable parameter set where, as noted by *Wood and Pellas* (1991), most of the parameters are unconstrained. In the absence of our knowledge of a "reasonable" parameter set for electromagnetic induction, the question of whether this can be the dominant heat source in the early solar system will remain unresolved. Electromagnetic induction continues to be invoked, particularly in scenarios where short-lived radionuclides do not produce the desired result.

1.2. Impact Heating

Impact energy is the heat generated when the gravitational potential energy of the impactor in the target's gravitational field (plus any kinetic energy associated with relative velocities due to orbital motion) is converted to heat. A portion of this heat is lost, carried off by escaping ejecta and/or radiated into space, and the remaining heat is deposited in the target asteroid. The gravitational potential energy of an impactor varies as the square of the target-body radius. *Melosh* (1990) pointed out that during accretion, when impact velocities are comparable to the target's escape velocity, the energy deposited by impacts on targets smaller than a critical radius is not significant, and that heat deposition by impacts is a significant cause of global metamorphism in planets, but insignificant for most asteroids.

Although impacts could not have caused global metamorphism of asteroids, they may well have caused localized heating that mimics the effects of thermal metamorphism. Impacts have commonly affected meteorites, and many ordinary chondrites have been shocked and subsequently annealed. These rocks possess olivines with sharp optical extinction (indicative of unshocked S1 material), but also include relict shock features such as extensive silicate darkening, shock veins, metallic Cu, and polycrystalline troilite. In the case of LL6 MIL 99301, the annealing event occurred 4.26 G.y. ago (*Dixon et al.,* 2003), ~300 m.y. after accretion. At this late epoch, impacts are the only plausible heat source. Proponents of impact heating believe the following to be consistent with the hypothesis: (1) the positive correlation between petrologic type and shock stage among ordinary chondrites; (2) the observation that, among the three ordinary chondrite groups, L chondrites have the highest (and H chondrites the lowest) proportions of highly annealed members and highly shocked members; and (3) the general trend for chondrite groups with many highly metamorphosed members (H, L, LL, EH, EL, CK) to also have shocked members of stage S4, and for chondrite groups with no highly metamorphosed members (CI, CM, CO, CR) to have no shocked members of stage S4 (*Rubin,* 2004). Proponents of impact heating, in addition, believe that it could have operated on porous rubble piles. In such bodies, collisional kinetic energy is distributed through relatively small volumes of material and efficiently converted into heat. Although impacts have clearly heated chondrites, this may be a localized annealing overprint rather than the thermal event that produced the metamorphic sequence in chondrites.

1.3. Heating by the Decay of Aluminum-26

In a landmark paper, *Lee et al.* (1976) observed a large anomaly in the isotopic composition of Mg in a Ca-Al-rich inclusion (CAI) from the Allende meteorite. *Lee et al.* (1976) hypothesized that the most plausible cause of the anomaly was the *in situ* decay of now-extinct ^{26}Al, and measured an initial ratio of ^{26}Al/^{27}Al equal to 5×10^{-5} at CAI formation. The numerical value of the following four parameters provided just the correct amount of heat to metamorphose asteroidal bodies for a few million years: (1) the proportional abundance of Al in chondrites, (2) the initial ratio, (3) the short half-life of ^{26}Al, and (4) the high decay energy per nucleon (2 MeV).The efficacy of the heat source dwindled rapidly because of the short half-life. Once the heat source dwindled in potency, the asteroidal bodies lost their heat

relatively quickly due to the large surface area to volume ratio. Thus, ^{26}Al was able to theoretically produce a short period of intense heating in the early solar system, as was being observed in meteorites.

For the last 30 years, ^{26}Al has largely dominated any discussion of asteroidal heating. The case for ^{26}Al has become increasingly stronger over the last decade. Some perceived problems with the ^{26}Al hypothesis (*Wood and Pellas,* 1991) have been addressed: Magnesium-26 due to the decay of ^{26}Al has been detected in noncumulate eucrites (*Srinivasan et al.,* 1999), and reasons as to why it might not be observed in others have been put forward (*Ghosh and McSween,* 1998; *LaTourrette and Wasserburg,* 1998). An explanation for the difference in ages between noncumulate and cumulate eucrites has been offered (*Ghosh and McSween,* 1998). The thermal stratification in the asteroid belt has been explained (*Grimm and McSween,* 1993; *Ghosh et al.,* 2001). A compilation of ^{26}Mg measurements for various meteorite types shows a conspicuous peak at the canonical value of ^{26}Al/^{27}Al of 5×10^{-5} (*MacPherson et al.,* 1995). However, the existence in certain refractory inclusions (e.g., FUN inclusions) of isotopic anomalies with no radiogenic excess of ^{26}Mg is perceived as a reason to invoke isotopic heterogeneity in the distribution of ^{26}Al (*MacPherson et al.,* 1995). The issue of possible nebular heterogeneity of ^{26}Al clouds its efficacy as a heat source; however, the consistency of ^{26}Al/^{27}Al ratios in CAIs and meteorites of different classes argues for homogeneity (*Huss et al.,* 2001).

1.4. Heating by Decay of Iron-60

Iron-60 was proposed as a heat source by *Shukolyukov and Lugmair* (1993) on the basis of measurements in Juvinas. Using relative chronology, they calculated the initial ratio of ^{60}Fe/^{56}Fe to be ~10^{-6} at the time of CAI formation. Because of the high abundance of Fe in the solar system and the high decay energy of ^{60}Fe (3.04 MeV), it was proposed that ^{60}Fe could be a planetary heat source. As of 1995 (G. Lugmair, personal communication), this ratio was revised downward to ~10^{-8}. *Ghosh* (1997) made a first-order calculation of the heat generated per kilogram due to decay of ^{26}Al and ^{60}Fe with initial ratios (at CAI formation) of 5×10^{-5} and 1×10^{-8}, respectively. The calculations show that the rate of heat generation at CAI formation is 1×10^{7} and 1×10^{3} J/m.y./kg for ^{26}Al and ^{60}Fe, respectively. In other words, if the initial ratio of ^{60}Fe/^{56}Fe was 1×10^{-8}, the rate of heat generation by ^{60}Fe is 4 orders of magnitude lower than that of ^{26}Al. This shows that the initial ratio of ^{60}Fe needs to be 4 orders of magnitude higher to be able to match heat production by ^{26}Al. A recent paper by *Mostefaoui* (2005) analyzed the mineral phases of troilite and magnetite in Semarkona (LL3) and reported an initial ratio of $0.92 \pm 0.24 \times 10^{-6}$ for ^{60}Fe/^{56}Fe. While this ranks among the higher published initial ratios of ^{60}Fe/^{56}Fe, the rate of heat generation at CAI formation for ^{60}Fe in such a scenario would still be 2 orders of magnitude lower than ^{26}Al. Thus, the state of our present knowledge calls for a limited role, if any, for ^{60}Fe heating; i.e., ^{60}Fe could not, for example, have been responsible for the early solar system heating by itself. Having said that, ^{60}Fe can have a secondary effect on planetary and asteroidal heating in two ways. First, ^{60}Fe may cause considerable heating when Fe is segregated in the core during core formation. *Ghosh* (1997) evaluated such a scenario for Vesta with an initial ratio of 1×10^{-8}, and failed to establish any significant heat generation by ^{60}Fe. It will be interesting to revisit the problem using the updated ^{60}Fe/^{56}Fe ratios reported recently by *Mostefaoui* (2005). Second, while ^{60}Fe cannot surpass rate of heat generation by ^{26}Al for the first few million years, it can moderate cooling rates by staying live for a longer time than ^{26}Al, since the half-life of ^{60}Fe is 1.5 m.y. (more than twice that of ^{26}Al).

The primary motivation of this chapter is to discuss the thermal stratification of the asteroid belt; a detailed review of heat sources is beyond the scope of the paper. For a more detailed discussion of thermal evolution models, see *McSween et al.* (2003); for a somewhat dated but otherwise excellent review of the plausibility of heat sources, see *Wood and Pellas* (1991).

2. THERMAL MODELING BASICS

The thermal evolution of the asteroid can be divided into the following stages: accretion, heating (with or without melting and differentiation, metamorphism, or aqueous alteration), and cooling. The heat transfer equation is the basis of the calculations [for detailed discussion of the equation and parameters, see appendix in *Ghosh and McSween* (1998)]: This is the standard diffusion equation with a diffusion term that equates the rate of temperature change to the heat lost by thermal conduction plus any heat generated by a heat source. The heat source term is different depending on the heat source or the combination of heat sources used. Most models assume asteroidal accretion to be instantaneous and heating to occur in a body of a fixed size. *Ghosh and McSween* (2000) presented a model for incremental accretion, in which the body's radius increases with time, and *Ghosh et al.* (2001) used growth rates from a dynamical accretion calculation (*Weidenschilling et al.,* 1997) in an incremental accretion thermal model. As with most theoretical problems, there are uncertainties in initial conditions (e.g., the temperature of the asteroid at the beginning of the simulation), boundary conditions (e.g., the nebular ambient temperature and the emissivity of the asteroid), and model parameters (e.g., specific heat capacity and thermal diffusivity, and their temperature and composition dependence). Although a methodical study has not been conducted, the parameters are tightly constrained in comparison to models of electromagnetic induction heating. Boundary conditions are implemented in two ways: The Dirichlet boundary condition forces the temperature of the surface of the asteroid to the temperature of the ambient nebula, and the radiation boundary condition calculates a heat flux depending on the difference in temperature be-

tween the asteroidal surface and the nebula. Although the radiation boundary condition is numerically unstable, it is believed to be more realistic (*Ghosh and McSween,* 1998). Three methods exist for numerical solution of the heat transfer: the classical series solution (e.g., *Miyamoto,* 1981; *Bennett and McSween,* 1996; *Akridge et al.,* 1998), the finite-difference method (e.g., *Wood,* 1979; *Grimm and McSween,* 1989), and the finite-element method (e.g., *Ghosh and McSween,* 1998). The finite-element method, which uses a basis function to minimize approximation error during numerical integration, has been found to be more accurate than either the finite-difference method or the classical series solution (*Baker and Pepper,* 1991).

3. THERMAL STRUCTURE OF THE ASTEROID BELT

An understanding of the thermal evolution of the asteroid belt is one of the most important problems of planetary science and one of its greatest challenges. An understanding of the evolution of the asteroid belt can help constrain the origin and early history of the solar system, the radial gradient in composition, the difference in the dynamical parameters with heliocentric distance, and the disruption of asteroidal bodies at a later stage.

Gradie and Tedesco (1982) showed that the asteroid belt is stratified with different asteroidal classes, as inferred from their photometric properties, distributed at different heliocentric distances. In particular, *Gradie and Tedesco* (1982) observed that asteroids with spectra indicative of high-temperature silicate minerals (like asteroid types E, R, S, M, F) are concentrated between 1.8 and 3 AU, while dark C-rich types (like asteroid types P, C, D) seem to be located farther away from the Sun.

Bell et al. (1989) attempted the first quantification of asteroid peak temperatures as a function of heliocentric distance; Fig. 1a shows the distribution of the various taxonomic types, and the distributions of different spectral classes are seen to peak at various locations in the asteroid belt. *Bell* (1986) assumed various spectral types to correspond to specific meteorite families. Using Tholen taxonomic classes, *Bell* (1986) grouped asteroids into three broader superclasses based on the inferred degree of heating and metamorphism. The three superclasses are: (1) primitive asteroids with little or no discernable evidence of heating; (2) metamorphosed asteroids that have undergone heating sufficiently to exhibit spectral changes; and (3) igneous asteroids whose mineralogy indicates derivation from igneous processes.

A plot of the abundance of superclasses with heliocentric distance (Fig. 1b) by *Bell* (1986) added to the realization that bodies with distinct thermal histories occur at different characteristic distances from the Sun, thereby restricting asteroid evolution models (e.g., *Zellner,* 1979; *Gradie and Tedesco,* 1982). Igneous asteroids dominate inward of 2.7 AU, metamorphosed asteroids around 3 AU, and ice-bearing planetesimals beyond 3.4 AU (*Gradie and Tedesco,* 1982; *Bell et al.,* 1989). The relative abundance of the igneous superclass of *Bell et al.* (1989) decreases from about 100% at ~2 AU to 0% at 3.4 AU, while the relative abundance of the primitive superclass increases from 0% to 100% from 2 AU to about 3.4 AU. The metamorphic class is more broadly distributed with a smaller peak of about 10% around 3 AU. There is some uncertainty attributable to orbital reshuffling, but an overall structure is preserved. Also, the quoted boundaries represent transition zones rather than clean lines of demarcation, since each taxonomic class defines a roughly Gaussian distribution with a full width of distribution at half maximum value (FWHM) of ~1 AU.

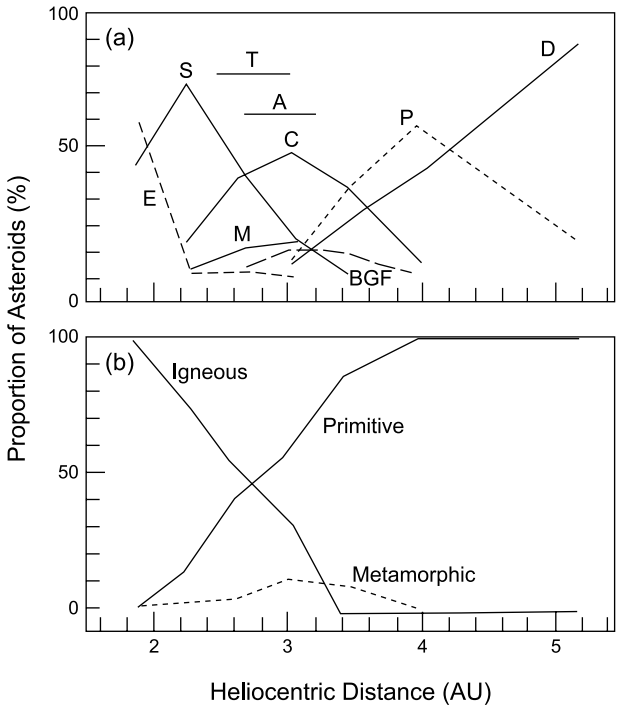

Fig. 1. **(a)** Distribution of various Tholen taxonomic types as a function of heliocentric distance. **(b)** Distribution of superclasses as a function of heliocentric distance. The diagram shows the predominance of melted asteroids in the inner belt and unaltered asteroids in the outer belt.

There have been a couple of realizations in this area since *Bell et al.* (1986) was published. First, *Bottke et al.* (2000) showed that dynamical models of meteorite delivery indicate that most of the sampled meteorite parent bodies lie near or inside the 5:2 resonance or at 2.82 AU. Thus, according to *Bottke et al.* (2000), the inner belt has been sampled in much greater detail in terrestrial meteorite collections. Second, *Keil* (2000) showed that 80% of the ~135 meteorite types in terrestrial collections underwent either partial or complete melting. The remaining 20% either underwent metamorphism or aqueous alteration.

Hardersen (2003), as part of his doctoral dissertation with M. Gaffey, undertook a more detailed mineralogic mapping of the asteroid belt by taking into account the latest

constraints from spectroscopy, dynamical models, and mineralogical studies of asteroids. He started by dividing asteroids into two classes: Class I asteroids, which allow diagnostic determinations of their mineralogy, and Class II asteroids, where the determination is nondiagnostic and open to interpretation. Out of the initial dataset of 152 asteroids, 44 were placed in the Class I group. The Class II asteroids include 32 S-type asteroids from *Gaffey et al.* (1993), 12 asteroids from *Jones et al.* (1990), and 56 C-, D- and T-type asteroids. Based on increasing heating, *Hardersen* (2003) divided the asteroids into four groups, Zones 0, I, II, III, and IV, respectively. *Hardersen* (2003) then tried to account for parent-body radii in evaluating the maximum temperatures possible. The results of *Hardersen* (2003) reinforce the idea of thermal stratification of the asteroid belt proposed by *Gradie and Tedesco* (1982) and *Bell et al.* (1989) except for regional heterogeneity superimposed on this overall trend.

The radial stratification of the asteroid belt would have been disturbed by the dynamical process(es) that removed most of its mass. This depletion may have blurred the primordial variation of compositions with heliocentric distance, but did not erase it. *Petit et al.* (2001) performed numerical integrations of orbits perturbed by Jupiter and massive planetary embryos. They showed that during excitation and depletion of the belt, surviving asteroids would have experienced changes in semimajor axis of several tenths of an AU, consistent with the observed transitions between regions dominated by taxonomic types S, C, and D. After depletion of the belt, the largest surviving bodies were too small to further alter asteroidal orbits by gravitational scattering. Later collisional evolution resulted in only minor dispersion of orbital elements of fragments, as shown by preservation of Hirayama families.

4. HELIOCENTRIC ZONATION IN A MODEL OF ALUMINUM-26 HEATING

Decrease of surface density of planetesimals from the inner to the outer asteroid belt coupled with time-dependent heating by ^{26}Al decay has been advocated to explain the heliocentric zonation (*Grimm and McSween,* 1993). The decrease in surface density with heliocentric distance results in a lower probability of bodies colliding with each other. The decreased likelihood of collisions in the outer belt translates to a slower accretion rate. This results in longer accretion times in the outer belt compared to the inner belt. Variable ^{26}Al heating would have occurred if the initial amount of ^{26}Al was uniform at the time of CAI formation, yet the amount incorporated into planetesimals was controlled by the time at which they accreted. *Grimm and McSween* (1993) assumed accretion to be instantaneous at a given distance (i.e., the asteroid formed at the instant the process of accretion was completed) on a timescale that increased from the inner to the outer belt. As a result, asteroids across the belt incorporated different amounts of live ^{26}Al and therefore underwent variable heating.

According to analytical models of planetary accretion (*Lissauer and Stewart,* 1993), the accretion rate is proportional to the mass in the accretion zone and inversely proportional to the square of the heliocentric distance and the width of the accretion zone (*Grimm and McSween,* 1993, equation (1)). Empirically, it can be stated that accretion time is proportional to the nth power of heliocentric distance a when n = 1.5–3, depending on the assumptions about the radial variations of surface density of the planetesimal swarm (*Grimm and McSween,* 1993), or $\tau = a^n$, for the usual assumption that surface density varied as $a^{-3/2}$, n = 3. Using the derived proportional relationship between accretion time and heliocentric distance, *Grimm and McSween* (1993) parameterized accretion time across the asteroid belt. According to the model, all asteroids at a specific heliocentric distance were assumed to have the same accretion time. The model assumed temperature-dependent properties of ice and rock and included thermodynamic effects of phase transitions. The silicate- and ice-melting isotherms were taken to be 1100°C and 0°C, and were assumed to have occurred at 2.7 AU and 3.4 AU, respectively. Two models were run: one without ice, and another with 30% ice. The results of the first case are illustrated in Fig. 2. The best fit was obtained for n = 3 and a formation time of 3.5 and 3 m.y. for asteroids at 2 AU, for anhydrous and hydrous models, respectively.

By assuming instantaneous accretion (i.e., asteroids with fixed sizes began thermal evolution after a time delay, rather than growing over that interval), however, *Grimm and McSween* (1993) neglected the dynamics of the accretion process as well as heat budgeting during planetesimal growth. As they acknowledged, the inclusion of radioactive heat *during* accretion would result in higher temperatures, thus the accretion times (peak temperatures) calculated bracket

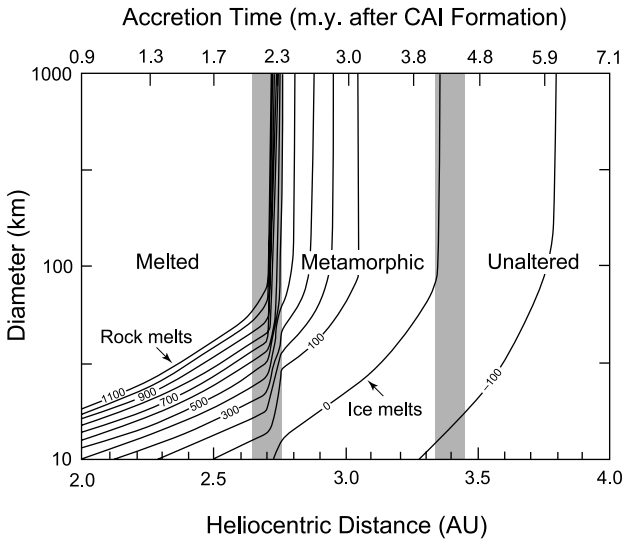

Fig. 2. Peak temperatures as a function of accretion time, heliocentric distance and asteroid radius for bodies that do not contain ice.

the upper bound (lower bound) of possibilities. Also, their results show that at 2 AU bodies of <~50 km radius would have a peak temperature of 870 K or less (the temperature threshold for type 4 metamorphism). Mass distributions from accretion codes (e.g., *Weidenschilling et al.,* 1997) show that bodies <~50 km radius would constitute a significant mass fraction at a particular heliocentric distance. Thus, the peak temperatures calculated for the inner asteroid belt by *Grimm and McSween* (1993) would yield a significant fraction of unaltered asteroids and not melted bodies as is observed. In principle, this problem could be alleviated by assuming a steeper gradient of accretion times with distance and shorter timescales in the main belt. However, the assumption of instantaneous accretion with a time delay is physically not justified.

5. HELIOCENTRIC ZONATION IN A MODEL OF ELECTROMAGNETIC INDUCTION HEATING

The discovery of the heliocentric zonation of the asteroid belt intuitively favored a heating agent with the Sun as an energy source. Thus, intuitively the intensity of solar wind should decrease with heliocentric distance, and this should moderate the heating that takes place with increasing heliocentric distance. Hence, electromagnetic induction heating models were favored initially to explain the thermal stratification of the asteroid belt. However, since electromagnetic induction heating is dependent on multiple parameters, the relationship between heliocentric distance and peak temperature is not that simple. To give an idea of the complexity, let us consider the peak temperatures attained as a function of heliocentric distance and planetesimal size. *Herbert et al.* (1991) made four runs with different parameter sets; in all these runs, bodies of a particular size bracket melted irrespective of heliocentric distance. What this means is, if the size of the body was larger or smaller than the size bracket for melting, irrespective of heliocentric distance, they would never melt. Also, this means that bodies of a particular size range would melt irrespective of heliocentric distance. Thus, it is important to highlight that electromagnetic induction heating proponents do not have an unambiguous model to explain the thermal stratification of the asteroid belt.

6. HELIOCENTRIC ZONATION IN A COMBINED ACCRETION-THERMAL MODEL

6.1. Methodology

As will be shown below, timescales for accretion of planetesimals in the asteroid region are on the same order as the decay timescale for ^{26}Al, thus the thermal evolution of parent bodies of meteorites is coupled to their accretionary history. The characteristic timescale for accretion increases with heliocentric distance, due to the lower surface density of accretable matter and longer orbital periods. These factors lead to differences in thermal histories between the inner and outer belt regions. In this section we evaluate the thermal histories of planetesimals as functions of size and heliocentric distance, using a numerical code for heat transfer and realistic growth rates derived from a numerical simulation of accretion. We use these results to derive a quantitative estimate of the mass fraction of material that experiences various degrees of thermal metamorphism at different locations within the asteroid belt.

6.2. Thermal Code

The thermal code tracks the heat budget of an accreting planetesimal, with production of heat by radioactive decay and transfer of heat by conduction, with a moving boundary condition as the body grows in size (*Ghosh et al.,* 2003). The dominant source of radiogenic heating is ^{26}Al, due to its short half-life and relatively high abundance; contributions by other nuclides are not taken into account since heat generated by them has been shown to be negligible (*Ghosh and McSween,* 1998). The initial abundance of ^{26}Al relative to ^{27}Al is 5×10^{-5} at the time of CAI formation (*Clayton,* 1999; *Huss et al.,* 2001). Accretion is assumed to initiate 2 m.y. after CAI formation (*Amelin and Krot,* 2002; *Russell et al.,* 2006). The rate of heat production decreases with time as the ^{26}Al decays. The initial composition and total Al abundance is taken to be that of H chondrites (*Ghosh and McSween,* 1998). Temperature-dependent specific heat capacity and the latent heat for melting are included (*Ghosh and McSween,* 1998, 1999). Where water ice is assumed to be present, the specific heat, latent heat of melting and vaporization, and heat of hydration (at 298 K) and dehydration (at 648 K) are incorporated from *Grimm and McSween* (1989). The thermal code is used to characterize the mass distribution of material with varying degrees of thermal metamorphism, according to the peak temperatures reached in the centers of planetesimals. Thus, we evaluate radius thresholds for planetesimals to remain unaltered (<870 K), metamorphose (870–1223 K), or undergo Fe-FeS melting (1223–1443 K), silicate melting (1443–2123 K), or complete melting (>2123 K). For bodies containing ice, the following thresholds are used: ice unmelted (<273 K), melted with aqueous alteration (273–648 K), and dehydrated (>648 K). For convenience, the respective bodies are notated as A, B, C, D, E for bodies without ice, and X, Y, Z for bodies with ice, respectively. The nebula is assumed to be optically thick, with temperature decreasing inversely with heliocentric distance. The presence of ice in the outer asteroid belt can be inferred from the spectral signatures of D and P asteroids (*Lebofsky et al.,* 1981), the textures of carbonaceous chondrites that are characteristic of aqueous alteration (*Bunch and Chang,* 1980), and the difficulty of condensing hydrous silicates directly from the nebula (*Prinn and Fegley,* 1987). The temperature is chosen so that water ice condenses (T = 160 K) at 3.4 AU. Thus, we introduce 30% by volume of ice in bodies that accrete beyond this distance (*Grimm and McSween,* 1989). The initial temperature of the kilometer-

sized starting bodies and the temperature of the accreted material are assumed to be equal to the temperature of the ambient nebula at any given distance. Accretion of material that condensed in a turbulent nebula would result in a mixture of unequilibrated grains. The low internal pressures within asteroid-sized bodies and the porosity of most meteorites (*Weidenschilling and Cuzzi,* 2006) argue for accretion of unconsolidated material. Thus, we assume the accreting planetesimals to have a thermal diffusivity characteristic of unsintered porous dust, taken to be 10^{-9} m^2 s^{-1} (*Fountain and West,* 1970). Sintering is a complex process occurring at high temperatures (as high at 1050°C for basalt powder) and dependent on static and shock pressures, composition, and the presence or absence of volatiles in voids. As temperature increases, the interior is expected to undergo sintering, but the surficial layers that govern heat loss from the interior would remain unsintered. Sintering of dust into rock could, in principle, increase the diffusivity by 2 orders of magnitude. This process is ignored in the present study since we are interested in peak temperatures that are attained primarily in the first few million years of accretion. Test calculations show that maximum interior temperatures are similar for bodies with the diffusivity of solid rock, provided a regolith of low diffusivity is present, compared to a body composed of unsintered dust.

6.3. Accretion Code

The evolution of the size distribution of the planetesimal swarm is calculated using an accretion code that computes rates of collisions and velocity evolution due to gravitational stirring among bodies in the swarm (*Weidenschilling et al.,* 1997). This calculation gives the size distribution as functions of both heliocentric distance and time. In this simulation, the initial bodies are assumed to be 0.5 km in radius at the start of accretion. The mass is assumed to be distributed with surface density inversely proportional to the heliocentric distance. The surface density of solid matter is chosen to be 8.3 g cm^{-2} at 1 AU, corresponding to a total mass of the swarm of nearly 4 $M_\oplus$ between 2 and 4 AU. These parameters are consistent with a solar nebula about 1.5× the minimum mass. The calculation assumes no fragmentation; i.e., all collisions result in coagulation, which yields a lower limit to the accretion timescale. Growth is fastest in the inner region, where surface density is high and orbital periods are shortest. The formation of large bodies occurs as a wave that propagates outward with time. The size distribution evolves with runaway growth of large bodies in the swarm of smaller bodies. This produces an "oligarchy" of protoplanetary embryos of masses ~10^{26}–10^{27} g (*Kokubo and Ida,* 1993), with comparable masses and roughly uniform orbital spacing. After 1 m.y. of accretion (3 m.y. after CAI formation), the asteroid region contains bodies with radii ranging from the original 0.5 km to ~2500 km (Fig. 3). The resulting mass distribution is bimodal, with comparable fractions of the total mass in the embryos and a tail of smaller bodies with an approximate

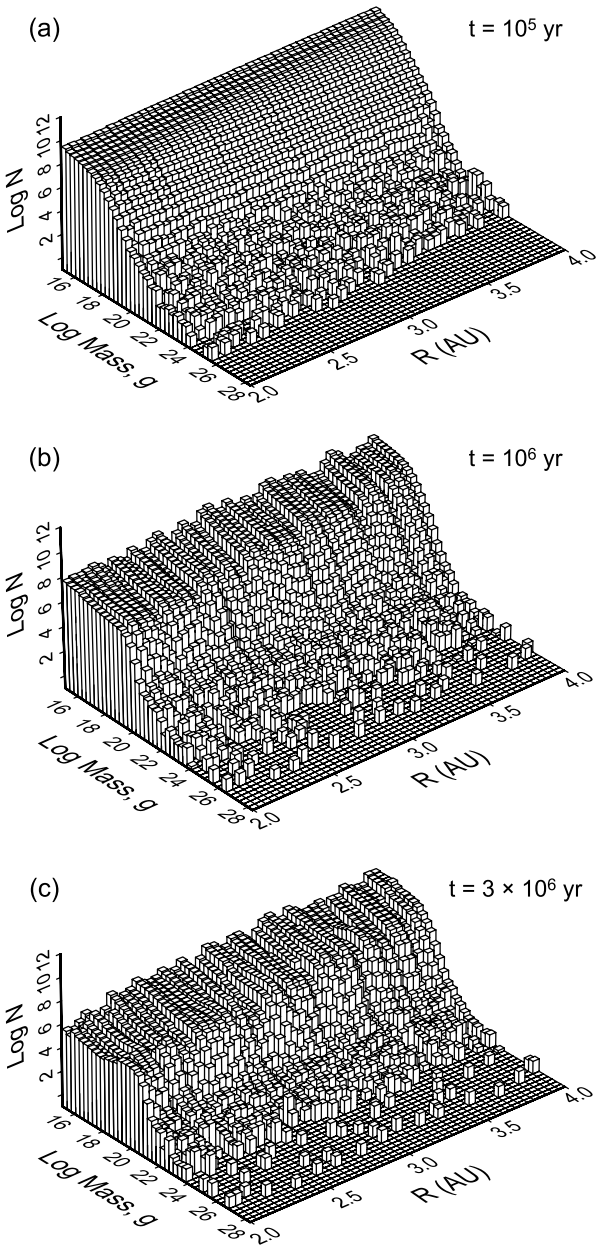

Fig. 3. Size distributions produced by the accretion code at model times of **(a)** 10^5, **(b)** 10^6, and **(c)** 3×10^6 yr from the start of accretion (assumed to be 2×10^6 yr after CAI formation).

power-law distribution at radii less than about 100 km. The present asteroid belt contains much less mass than is present in this simulation (by 3 orders of magnitude), and with the exception of Ceres, Pallas, and Vesta, it consists of bodies of radii <~200 km. Most of the original mass, and all the larger embryos, are believed to have migrated to jovian resonances and were eventually removed by collisions with terrestrial planets or encounters with Jupiter (*Chambers and Wetherill,* 2001). Only the small remnant of a formerly much more numerous population is present in the current asteroid belt to act as the source of meteorites.

6.4. Combining the Results

Growth rates at various heliocentric distances are estimated from the multizone accretion code, and these are used in the thermal evolution code to compute internal temperature profiles. At any given time, the size distribution contains bodies with a range of radii, which have grown at different rates due to the stochastic nature of collisional coagulation. The rate of change of radius of planetesimals (dR/dt) depends on the mass bin; on average, a 200-km body has grown at twice the rate of a 100-km body with the same semimajor axis, with the rate varying with heliocentric distance. For simplicity, the growth of any body's radius is assumed to be linear in time when computing its thermal profile. This assumption ignores the possibility that two bodies of the same size could be produced by different series of collisions, with growth rates that differ in detail. Such stochastic effects, and differences in heliocentric distance, may explain why Vesta experienced melting while the larger Ceres does not appear to be differentiated. In comparing the results of simulations of early evolution of the belt and the currently observable asteroids, it is necessary to consider both the depletion in mass and the effects of ~4.5 G.y. of collisional evolution that occurred after eccentricities and inclinations were stirred up to their current high values. All the large embryos, which would have been melted by ^{26}Al, have been removed. Of the remainder, a significant fraction of mass would have been in the smallest bodies (radii <20 km). Collisional evolution is believed to have preferentially removed these small asteroids. Simulations of model asteroid populations predict that bodies of initial radius less than a specific threshold, ~10–20 km, would be destroyed by collisional fragmentation over the age of the solar system (*Davis et al.,* 1989). The present population of small asteroids in this size range consists of fragments of larger parent bodies, of original radii greater than the radius threshold for destruction by fragmentation. This collisional evolution and destruction of small primordial asteroids accounts for the near-ubiquity of thermal and aqueous alteration in meteorites and the lack of truly pristine material. Thus, *Ghosh et al.* (2001) assume that planetesimals of radius <14.5 km were destroyed by fragmentation, in computing the composition of the asteroid belt as a function of heliocentric distance. Similarly, larger asteroids >240 km are assumed to have migrated to the terrestrial planet region.

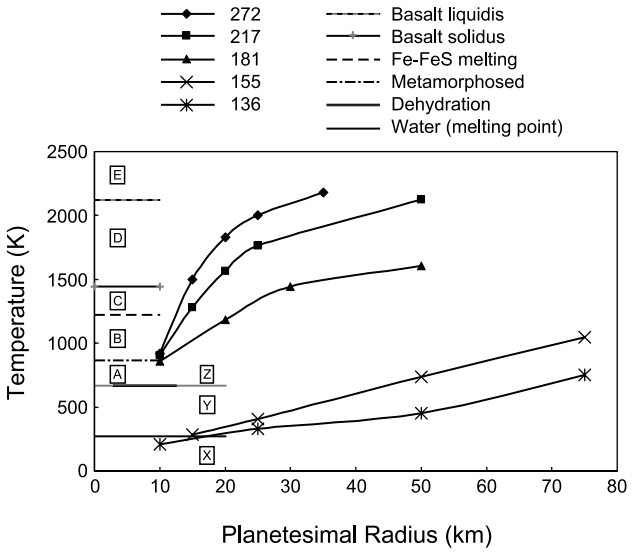

Fig. 4. Plots of maximum temperature realized in the interior of planetesimal against radius of the body. Accretion rates are constrained from *Weidenschilling et al.* (1997). An optically thick nebula with temperature inversely proportional to heliocentric distance is assumed, thus initial temperature of the planetesimals is assumed to decrease from 272 K at 2 AU to 136 AU at 4 AU. Condensation of ice is assumed to take place at approximately 3.4 AU, thus all planetesimals outward of 3.4 AU are assumed to contain 30% ice. The maximum temperature attained at a planetesimal center is calculated as a function of planetesimal radius for each heliocentric distance. These plots are then used to demarcate planetesimals at each heliocentric distance according to thermal regimes, i.e., the radius ranges of planetesimal types A–E and X–Z are evaluated. Planetesimals types A, B, C, D, and E are defined to represent the following thermal regimes: unaltered (<870 K), metamorphosed (870–1223 K), FeS melted (1223–1443 K), silicate melted (1443–2123 K), and totally molten (>2123 K). X, Y, Z indicate a corresponding scale for ice-bearing planetesimals: ice unmelted (<273 K), ice melted with subsequent aqueous alteration (273–648 K), and dehydrated (>648 K), respectively.

6.5. Results

At a specific heliocentric distance, the maximum temperature realized in the asteroid center increases with body size (Fig. 4). This is due to the decrease in the surface area to volume ratio as the size of the asteroid increases. On the other hand, peak temperatures for an asteroid of a given size decrease with heliocentric distance (Fig. 4). Using the data of peak temperature as a function of heliocentric distance and body size from Fig. 4, *Ghosh et al.* (2001) computed radius windows for planetesimal types A, B, C, D, E, X, Y, and Z. Using the radius windows, the mass distributions of the multizone accretion code are categorized according to the thermal history. This result translates into radial zoning of compositions, summarized in Fig. 5. The innermost asteroid belt shows a predominance of type D (or melted) planetesimals. At 3 AU, a predominance of type B (or metamorphosed) planetesimals is observed. Correspondingly, planetesimals with ice in the outer asteroid belt (3.4–4 AU) either undergo aqueous alteration or remain unaltered, if internal temperatures do not rise above the melting point of water. The compositional boundaries are not sharp, due to the distribution of sizes at any distance; these would be further blurred by orbital migration due to gravitational scattering that occurred before the removal of the larger protoplanetary embryos.

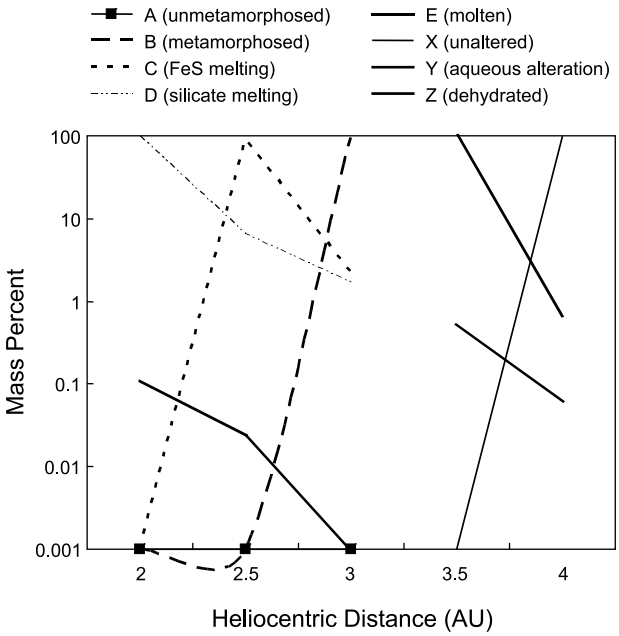

Fig. 5. Mass proportion of various planetesimal types as a function of heliocentric distance. Using the radius ranges for each planetesimal type calculated from Fig. 2, the mass distribution of the multizone accretion code is characterized in terms of planetesimal types. Bodies of radius <14.5 km are assumed to be destroyed by fragmentation. Bodies of radius >231 km are assumed to migrate to the terrestrial planet region. The histogram shows a predominance of melted planetesimals (type D) at 2 AU, FeS melted planetesimals (type C) at 2.5 AU, metamorphosed planetesimals (type B) at 3 AU, ice melted with subsequent aqueous alteration (type Y) at 3.5 AU, and ice unmelted (type X) at 4 AU.

6.6. Discussion

The following discussion examines each of the factors in the model to discern whether they are required to simulate (or, in contrast, serve to merely facilitate) the observed heliocentric zonation in the asteroid belt.

6.6.1. Fragmentation. The nature of accretion in the asteroid belt is such that a significant proportion of the mass remains in smaller size bins after the growth of large embryos. In the thermal model, it is not possible to sustain metamorphism in bodies <~10 km radius, due to the high surface area to volume ratio, which results in efficient removal of heat by radiation. Unless most of these bodies were removed by fragmentation, a substantial amount of the mass in all parts of the belt would consist of primitive, unaltered material. Yet the inner asteroid belt, according to observation, is dominated by melted or metamorphosed bodies. Thus, the only way to reproduce the radial stratification is to remove the smaller bodies by fragmentation.

6.6.2. Effect of nebular temperature. A temperature gradient is expected between the inner and outer asteroid belt, depending upon the assumed total mass of the nebula, its evolutionary stage, and the rate and scale of heat and mass transport by convective processes (*Boss,* 1996; *Cassen,* 1994). A temperature gradient is required to explain the presence of ice in the outer asteroid belt. The presence of ice in the present model is critical in reproducing the observed stratification, as explained in the next paragraph. However, the nature of the decrease in temperature with heliocentric distance is not a critical factor. In the thermal evolution model, we assume the initial bodies and accreted material to have temperatures corresponding to ambient conditions in an optically thick nebula, with T inversely proportional to heliocentric distance and with the ice line (T = 160 K) at 3.4 AU. If instead we assume the nebula to be optically thin, with T varying as $R^{-0.5}$, and keeping the same temperature of 160 K at 3.4 AU, the ambient temperature at 2 AU decreases from 272 K to 208 K. This decrease in temperature causes only a slight shift in peak temperature realized at the asteroid centers (Fig. 4), and a small change in the radius thresholds of various planetesimal types. In other words, the temperature gradient must allow the presence of ice in the outer asteroid belt; however, the exact nature of temperature decrease is not a critical factor in explaining the stratification.

6.6.3. Effect of ice. The incorporation of ice in asteroids produces thermal buffering because of greater specific heats of ice and water relative to silicates, dilution of the mass fraction of ^{26}Al, heats of melting and vaporization, and the endothermic dehydration reaction (*Grimm and McSween,* 1989). Approximately 3 kJ/g of energy is required to melt and vaporize ice, compared to ~1.6 kJ/g required to heat silicates from 200 to 1400 K (*Wood and Pellas,* 1991). In the absence of ice, the peak temperature for a 10-km-radius planetesimal at 4 AU would have exceeded 700 K, greater than the dehydration temperature of serpentine at ~648 K. This is contrary to spectral observations, which show evidence of aqueous alteration in the outer belt and the presence of water of hydration. Thus, inclusion of ice in the thermal model is critical in terms of reproducing the observed stratification.

6.6.4. Effect of sintering. A model run assuming a planetesimal to have the diffusivity of compacted rock calculates the radius threshold for melting and metamorphism at 2 AU of 51 km and 55 km, respectively. Due to the nature of the mass distribution that retains the median mass in smaller size bins, this translates into a predominance of unaltered bodies in the inner asteroid belt. It is not possible to offset this result unless the radius threshold for fragmentation is increased to ~50 km. However, literature on collisional evolution of asteroids (*Davis et al.,* 1989) indicates that bodies with primordial radii larger than 20 km should have survived. Therefore, unsintered bodies, or at least a significant thickness of regolith with low thermal diffusivity, is required.

6.6.5. Effect of the accretion process and the nature of aluminum-26 heating. The characteristic growth rate is proportional to the surface density of accretable matter and

the local Kepler frequency (*Lissauer and Stewart,* 1993). Thus, the physics of the accretion process requires faster accretion rates at smaller heliocentric distances; for the nominal model this difference is more than a factor of 5 between the inner and outer edges of the belt. Heating by ^{26}Al with a half-life of 0.7 m.y. acts in conjunction with faster accretion times in the inner asteroid belt to produce higher temperatures within planetesimals in the inner belt (*Grimm and McSween,* 1993). Heat generated during the accretion process decreases by more than an order of magnitude in 3 m.y., thus differences in accretion rates result in greater heat deposition for planetesimals accreting in the inner belt. This in turn results in greater heating in the inner belt in contrast to the outer belt. Had the accretion timescale been much longer or shorter than the half-life of the dominant heat source, the difference in thermal histories would be much smaller.

7. CONCLUSIONS AND FUTURE WORK

Many aspects of the asteroid belt evolution remain unclear. It is possible that the dynamical evolution of the belt, for example, did disrupt the primordial stratification. Thus, it is possible that what we see today does not resemble the initial configuration. However, at a minimum, it is well established that we have melted or metamorphosed asteroids in the inner belt and ice in the outer belt, thus there was at least a rudimentary form of thermal stratification.

Given the uncertainty in parameters of electromagnetic induction heating models (*Wood and Pellas,* 1991), it is probably premature to attribute the stratification to the effect of this mechanism (*Sonett et al.,* 1968; *Herbert,* 1989). Indeed, in certain induction models (*Herbert,* 1989), the relationship between heating and heliocentric distance is so weak that melting is produced throughout the belt, if at all. Also, in a model of electromagnetic induction heating, where planetesimals of a certain size bracket undergo heating (*Herbert,* 1989), smaller planetesimals would remain unmetamorphosed. This will produce the problem of an overabundance of unaltered bodies in the inner belt (although the subsequent collisional depletion of small bodies would also aid this model).

Thermal stratification of the asteroid belt was the result of the interplay of multiple processes. Integrated thermal-accretion models are the first step in trying to realistically simulate how the stratification was produced. Present models (*Ghosh et al.,* 2001) tie the structure of the asteroid belt to a dynamically plausible accretion history, and show that a combination of several factors is required to reproduce its radial compositional stratification. The factors critical to reproducing the stratification are slower accretion in the outer belt combined with decreasing abundance of ^{26}Al with time and low thermal diffusivity of unsintered planetesimals. Temperatures in the asteroid belt should have allowed for condensation of ice in the outer belt; however, the actual temperature gradient is not critical. It is also necessary to allow for the removal of large planetary embryos (as well as most of the original mass at all sizes) by gravitational scattering after the accretionary era, and the selective collisional depletion of small planetesimals of primitive composition over the lifetime of the solar system. A significant improvement in our understanding of the processes that cause the stratification can be attained if nebular models can be anchored to CAI formation. This would enable an integration of nebular models with thermal and accretion models. In addition to providing accurate temperatures of the accreting mass and the ambience, it will constrain the rate at which solids condense in the terrestrial planet region. This is turn will constrain accretion models, which at present assume that the entire mass in the terrestrial planet region existed at the start of the simulation.

Acknowledgments. This work was supported by NASA grants NASG-54387 (H.Y.M.), Center for Innovative Technology Challenge Grant (A.G.), NAGW-4219 (S.J.W.), and NAG5-4766 (A.E.R.). We thank the Joint Institute for Computational Science at the University of Tennessee and the NASA HPCC/ESS Program for the use of computer time.

REFERENCES

Akridge G., Benoit P. H., and Sears D. W. G. (1998) Regolith and megaregolith formation of H-chondrites: Thermal constraints on the parent body. *Icarus, 132,* 185–194.

Amelin Y. and Krot A. N. (2002) Pb isotopic age of chondrules from CR carbonaceous chondrites ACFER 059. *Meteoritics & Planet. Sci., 37,* A12.

Baker A. J. and Pepper D. W. (1991) *Finite Element 1-2-3.* McGraw-Hill, New York.

Bell J. F. (1986) Mineralogical evolution of meteorite parent bodies (abstract). In *Lunar and Planetary Science XVII,* p. 985. Lunar and Planetary Institute, Houston.

Bell J. F., Davis D. R., Hartmann W. K., and Gaffey M. J. (1989) Asteroids: The big picture. In *Asteroids II* (R. P. Binzel et al., eds.), pp. 921–945. Univ. of Arizona, Tucson.

Bennett M. E. III and McSween H. Y. Jr. (1996) Revised model calculations for the thermal histories of ordinary chondrite parent bodies. *Meteoritics, 31,* 783.

Boss A. P. (1996) Evolution of the solar nebula. III. Protoplanetary disks undergoing mass accretion. *Astrophys. J., 469,* 906.

Bottke W. F. Jr., Rubincam D. P., and Burns J. A. (2000) Dynamical evolution of main belt asteroids: Numerical simulations incorporating planetary perturbations and Yarkovsky thermal forces. *Icarus, 145,* 301–331.

Bunch T. E. and Chang S. (1980) Carbonaceous chondrites. II — Carbonaceous chondrite phyllosilicates and light element geochemistry as indicators of parent body processes and surface conditions *Geochim. Cosmochim. Acta, 44,* 1543.

Cassen P. (1994) Utilitarian models of the solar nebula. *Icarus, 112,* 405–429.

Chambers J. E. and Wetherill G. W. (2001) Planets in the asteroid belt. *Meteoritics & Planet. Sci., 36,* 381–399.

Clayton D. D. (1980) Chemical energy in cold-cloud aggregates — The origin of meteoritic chondrules. *Astrophys. J. Lett., 239,* L37–L41.

Clayton R. N. (1999) Oxygen isotope studies of carbonaceous chondrites. *Geochim. Cosmochim. Acta, 63,* 2089.

Davis D. R., Weidenschilling S. J., Farinella P., Paolicchi P., and Binzel R. P. (1989) Asteroid collisional history: Effects on sizes and spin. In *Asteroids II* (R. P. Binzel et al., eds.), pp. 805–826. Univ. of Arizona, Tucson.

DeCampli W. M. (1981) T Tauri winds. *Astrophys. J., 244,* 124–146.

Dixon E. T., Bogard D. D., and Rubin A. E. (2003) ^{39}Ar-^{40}Ar evidence for an ~4.26 Ga impact heating event on the LL parent body (abstract). In *Lunar and Planetary Science XXXIV,* Abstract #1108. Lunar and Planetary Institute, Houston (CD-ROM).

Edwards S., Cabrit D., Strom S. E., Heyer I., Strom K. M., and Anderson E. (1987) Forbidden line and Hα profiles in T Tauri star spectra: A probe of anisotropic mass outflows and circumstellar disks. *Astrophys. J., 321,* 473–495.

Fountain J. A. and West E. A. (1970) Thermal conductivity of particulate basalt as a function of density in simulated lunar and martian environments. *J. Geophys. Res., 75,* 4063–4069.

Gaffey M. J., Burbine T. H., and Binzel R. P. (1993). Asteroid spectroscopy: Progress and perspectives. *Meteoritics, 28,* 161–187.

Ghosh A. (1997) A thermal model for the differentiation of asteroid 4 Vesta based on radiogenic and collisional heating. Ph.D. dissertation, Univ. of Tennessee, Knoxville.

Ghosh A. and McSween H. Y. Jr. (1998) A thermal model for the differentiation of asteroid 4 Vesta, based on radiogenic heating. *Icarus, 134,* 187–206.

Ghosh A. and McSween H. Y. Jr. (1999) Temperature dependence of specific heat capacity and its effect on asteroid thermal models. *Meteoritics & Planet. Sci., 34,* 121–127.

Ghosh A. and McSween H. Y. Jr. (2000) The effect of incremental accretion on the thermal modeling of asteroid 6 Hebe. *Meteoritics & Planet. Sci., 35,* A59.

Ghosh A., Weidenschilling S. J., and McSween H. Y. Jr. (2001) Thermal consequences of the multizone accretion code on the structure of the asteroid belt (abstract). In *Lunar and Planetary Science XXXII,* Abstract #1760. Lunar and Planetary Institute, Houston (CD-ROM).

Ghosh A., Weidenschilling S. J., and McSween H. Y. Jr. (2003) Importance of the accretion process in asteroidal thermal evolution: 6 Hebe as an example. *Meteoritics & Planet. Sci., 38,* 711–724.

Gradie J. C. and Tedesco E. F. (1982) Compositional structure of the asteroid belt. *Science, 216,* 1405–1407.

Grimm R. E. and McSween H. Y. Jr. (1989) Water and the thermal evolution of carbonaceous chondrite parent bodies. *Icarus, 82,* 244–280.

Grimm R. E. and McSween H. Y. Jr. (1993) Heliocentric zoning of the asteroid belt by aluminum-26 heating. *Science, 259,* 653–655.

Hardersen P. S. (2003) Near-IR reflectance spectroscopy of asteroids and study of the thermal history of the main asteroid belt. Ph.D. dissertation, Rensselaer Polytechnic Institute, Troy, New York. 387 pp.

Herbert F. (1989) Primoridal electrical induction heating of asteroids. *Icarus, 78,* 402–410.

Herbert F., Sonett C. P., and Gaffey M. (1991) Protoplanetary thermal metamorphism: The hypothesis of electromagnetic induction in the protosolar wind. In *The Sun in Time* (C. P. Sonett et al., eds.), pp. 710–739. Univ. of Arizona, Tucson.

Huss G. R., MacPherson G. J., Wasserburg G. J., Russell S. S., and Srinivasan G. (2001) Aluminum-26 in calcium-aluminum-rich inclusions and chondrules from unequilibrated ordinary chondrites. *Meteoritics & Planet. Sci., 36,* 975–1025.

Jones T. D., Lebofsky L. A., Lewis J. S., and Marley M. S. (1990). The composition and origin of the C, P, and D asteroids: Water as a tracer of thermal evolution in the outer belt. *Icarus, 88,* 172–192.

Keil K. (2000) Thermal alteration of asteroids: Evidence from meteorites. *Planet. Space Sci., 48,* 887–903.

Kokubo E. and Ida S. (1993) Velocity evolution of disk stars due to gravitational scattering by giant molecular clouds. *Back to the Galaxy, Proceedings of the 3rd October Astrophysics Conference* (S. S. Hold and F. Verter, eds.), p. 380. AIP Conference Proceedings 278, American Institute of Physics, New York.

Kuhi L. V. (1964) Mass loss from T Tauri stars. *Astrophys. J., 140,* 1409.

LaTourrette T. and Wasserburg G. J. (1998) Mg diffusion in anorthite: Implications for the formation of early solar system planetesimals *Earth. Planet. Sci. Lett., 158,* 91–108.

Lebofsky L. A., Feierberg M. A., Tokunaga A. T., Larson H. P., and Johnson J. R. (1981) *Icarus, 48,* 453.

Lee T., Papanastassiou D. A., and Wasserburg G. J. (1976) Demonstration of ^{26}Mg excess in Allende and evidence for ^{26}Al. *Geophys. Res. Lett., 3,* 41–44.

Lissauer J. J. and Stewart G. R. (1993) Planetary accretion in circumstellar disks. In *Planets Around Pulsars*, pp. 217–233. California Institute of Technology, Pasadena.

Macpherson G., Davis A. M., and Zinner E. K. (1995) The distribution of aluminum-26 in the early solar system — A reappraisal. *Meteoritics, 30,* 365–386.

McSween H. Y. Jr., Ghosh A., Grimm R. E., Wilson L., and Young E. D. (2003) Thermal evolution models of asteroids. In *Asteroids III* (W. F. Bottke Jr. et al., eds.), pp. 559–571. Univ. of Arizona, Tucson.

Melosh H. J. (1990) Giant impacts and the thermal state of the early Earth. In *Origin of the Earth* (H. E. Newsom and J. H. Jones, eds.), pp. 69–84. Oxford Univ., New York.

Miyamoto M., Fujii N., and Takeda H. (1981) Ordinary chondrite parent body: An internal heating model. *Proc. Lunar Planet. Sci. 12A,* pp. 1145–1152.

Mostefaoui S., Lugmair G. W., and Hoppe P. (2005) ^{60}Fe: A heat source for planetary differentiation from a nearby supernova explosion. *Astrophys. J., 625,* 271–277.

Petit J.-M., Morbidelli A., and Chambers J. (2001) The primordial excitation and clearing of the asteroid belt. *Icarus, 153,* 338–347.

Prinn R. G. and Fegley B. Jr. (1987) The atmospheres of Venus, Earth, and Mars — A critical comparison. *Annu. Rev. Earth Planet. Sci., 15,* 171.

Rubin A. E. (2004) Postshock annealing and postannealing shock in equiliubrated ordinary chondrites: Implications for the thermal and shock histories of chondritic asteroids. *Geochim. Cosmochim. Acta, 68,* 673–689.

Russell S. S., Hartmann L., Cuzzi J., Krot A. N., Gounelle M., and Weidenschilling S. (2006) Timescales of the solar protoplanetary disk. In *Meteorites and the Early Solar System II* (D. S. Lauretta and H. Y. McSween Jr., eds.), this volume. Univ. of Arizona, Tucson.

Shimazu H. and Terasawa T. (1995) Electromagnetic induction heating of meteorite parent bodies by the primordial solar wind. *J. Geophys. Res., 100,* 16,923–16,930.

Shukolyukov A. and Lugmair G. W. (1993) Live iron-60 in the early solar system. *Science, 259,* 1138–1142.

Sonett C. P. and Colburn D. S. (1968) The principle of solar wind induced planetary dynamos. *Phys. Earth Planet. Inter., 1,* 326–346.

Sonnett C. P., Colburn D. S., and Schwartz K. (1968) Electrical heating of meteorite parent bodies and planets by dynamo induction from a premain sequence T Tauri "solar wind." *Nature, 219,* 924–926.

Srinivasan G., Goswami J. N., and Bhandari N. (1999) ^{26}Al in eucrite Piplia Kalan: Plausible heat source and formation chronology. *Science, 284,* 1348–1350.

Urey H. (1955) The cosmic abundances of potassium, uranium, and thorium and the heat balances of the Earth, the Moon and Mars. *Proc. Natl. Acad. Sci. U.S., 41,* 127–144.

Wasson J. T. (1974) *Meteorites: Classification and Properties.* Springer-Verlag, New York. 327 pp.

Weidenschilling S. J. and Cuzzi J. N. (2006) Accretion dynamics and timescales: Relation to chondrites. In *Meteorites and the Early Solar System II* (D. S. Lauretta and H. Y. McSween Jr., eds.), this volume. Univ. of Arizona, Tucson.

Weidenschilling S. J., Spaute D., Davis D. R., Mazari F., and Ohtsuki K. (1997) Accretional evolution of a planetesimal swarm 2. The terrrestrial zone. *Icarus, 128,* 429–455.

Wood J. A. (1979) Review of the metallographic cooling rates of meteorites and a new model for the planetesimals in which they formed. In *Asteroids* (T. Gehrels, eds.), pp. 740–760. Univ. of Arizona, Tucson.

Wood J. A. and Pellas P. (1991) What heated the meteorite parent planets. In *The Sun in Time* (C. P. Sonett et al., eds.), pp. 740–760. Univ. of Arizona, Tucson.

Zellner B. (1979) Asteroid taxonomy and the distribution of the compositional types. In *Asteroids* (T. Gehrels, eds.), pp. 783–806. Univ. of Arizona, Tucson.